

Abraham Model Correlations for Triethylene Glycol Solvent Derived from Infinite Dilution  
Activity Coefficient, Partition Coefficient and Solubility Data Measured at 298.15 K

Igor A. Sedov<sup>a</sup>, Timur I. Magsumov<sup>a</sup>, Erin Hart<sup>b</sup>, Ashley M. Ramirez<sup>b</sup>, Sarah Cheeran<sup>b</sup>, Maribel Barrera<sup>b</sup>, Melissa Y. Horton<sup>b</sup>, Anisha Wadawadigi<sup>b</sup>, Olivia Zha<sup>b</sup>, Xin Y. Tong<sup>b</sup>, William E. Acree, Jr.<sup>b</sup> and Michael H. Abraham<sup>c</sup>

<sup>a</sup> Department of Chemistry, Kazan Federal University, Kremlevskaya 18, Kazan 420008, Russia

<sup>b</sup> Department of Chemistry, University of North Texas, 1155 Union Circle Drive #305070,  
Denton, TX 76203 (USA)

<sup>c</sup> Department of Chemistry, University College London, 20 Gordon Street, London WC1H 0AJ  
(UK)

**Abstract**

A gas chromatographic headspace analysis method was used to experimentally determine gas-to-liquid partition coefficients and infinite dilution activity coefficients for 29 liquid organic solutes dissolved in triethylene glycol at 298.15 K. Solubilities were also determined at 298.15 K for 23 crystalline nonelectrolyte organic compounds in triethylene glycol based on spectroscopic absorbance measurements. The experimental results of the headspace chromatographic and spectroscopic solubility measurements were converted to gas-to-triethylene glycol and water-to-triethylene glycol partition coefficients, and molar solubility ratios using standard thermodynamic relationships. Expressions were derived for solute transfer into triethylene glycol by combining our measured experimental values with published literature data. Mathematical correlations based on the Abraham model describe the observed partition coefficient and solubility data to within 0.16 log<sub>10</sub> units (or less).

**Key Words and Phrases:** Infinite dilution activity coefficients; Molar solubility ratios; Headspace chromatographic analysis; Partition Coefficients; Solute transfer processes

---

\*To whom correspondence should be addressed. (E-mail: [acree@unt.edu](mailto:acree@unt.edu)); fax: 940-565-4318.

## Introduction

Growing environmental concern, combined with increased governmental regulations regarding organic waste disposal, has encouraged the chemical manufacturing sector to explore sustainable approaches in process design. Chemical manufacturers are encouraged to replace hazardous organic solvents with safer chemical alternatives. Replacement of toxic, flammable and environmentally harmful solvents is not an easy task. The physical properties and arrangement of functional groups in the organic solvent that give rise to the undesired health and environmental effects are often linked to the desired properties that are needed in the manufacturing process or application. For example, volatile organic solvents facilitate solvent recycling through fractional distillation. The large solvent pressure is a desired property in fractional distillation; however, this also leads to undesired air pollution and increased worker exposure to potentially toxic chemical vapors. Polar organic solvents containing the amide functional group are able to dissolve a wide range of polar organic starting materials needed in organic syntheses. However, the amide functional group can result in reproductive toxicity. Several excellent review articles and recent papers have been written concerning solvent selection and the use of environmentally friendly, green solvents in chemical synthesis and chemical separation processes. [1-8] The review articles contain lists of several harmful solvents, as well as recommended replacement solvents.

Our contribution in the area of solvent replacement has been to characterize the solubilizing properties of more than 100 different organic solvents [9-14], binary aqueous-methanol [15] and aqueous-ethanol solvent mixtures [16, 17], and 70 different ionic liquids [18] through experimental measurements and developing mathematical expressions that correlate the molar solubility, and both gas-to-organic solvent and water-to-organic solvent partition coefficients of dissolved solutes. Solubilization is an important consideration in selecting an

appropriate solvent for chemical extractions and recrystallization methods. Extractions and recrystallization are common industrial processes used to remove unwanted impurities from the desired chemical product. We have developed mathematical correlations for both hazardous organic solvents and potential solvent replacements. Our obtained expressions for solubility ratios and partition coefficients are based on the Abraham solvation parameter model which describes solute transfer between two condensed phases [9, 19-22]:

$$\log_{10} (P \text{ or } C_{S,\text{organic}}/C_{S,\text{water}}) = c_p + e_p \cdot \mathbf{E} + s_p \cdot \mathbf{S} + a_p \cdot \mathbf{A} + b_p \cdot \mathbf{B} + v_p \cdot \mathbf{V} \quad (1)$$

or solute transfer to an organic solvent from the gas phase:

$$\log_{10} (K \text{ or } C_{S,\text{organic}}/C_{S,\text{gas}}) = c_k + e_k \cdot \mathbf{E} + s_k \cdot \mathbf{S} + a_k \cdot \mathbf{A} + b_k \cdot \mathbf{B} + l_k \cdot \mathbf{L} \quad (2)$$

The dependent variables on the left-hand side of Eqns. 1 and 2 are the logarithm of the water-to-organic solvent partition coefficient,  $\log_{10} P$ , logarithm of the gas-to-organic solvent partition coefficient,  $\log_{10} K$ , or logarithms of molar solubility ratios,  $\log_{10} (C_{S,\text{organic}}/C_{S,\text{water}})$  and  $\log_{10} (C_{S,\text{organic}}/C_{S,\text{gas}})$ . The three concentrations denote the molar solubility of the solute in the respective organic solvent,  $C_{S,\text{organic}}$ , and in water,  $C_{S,\text{water}}$ , and a gas phase concentration of the solute,  $C_{S,\text{gas}}$ , respectively.

The independent variables in Eqns. 1 and 2 pertain to both solute properties (**E, S, A, B, V** and **L**) and the complimentary solvent/process properties ( $c_p, e_p, s_p, a_p, b_p, v_p, c_k, e_k, s_k, a_k, b_k$  and  $l_k$ ). Solute and solvent/process properties are defined in the Glossary of Symbols. Characterization of the solubilizing properties of organic solvents through development of Abraham model correlations aids in the solvent selection process. Once the coefficients have been determined for a given solvent or partitioning system one can calculate partition coefficients and solubility ratios for more than 8,000 different solutes simply by substituting the known equation

coefficients and solute descriptor values into eqns. 1 and 2 [23]. Principal Component Analysis on the solvent or equation coefficients allows one to identify solvents having similar solubilizing-related properties. One of our earlier publications [10] found that the solubilizing-related properties of diethylene glycol lie between those of ethylene glycol and 2-methoxyethanol. Of the three organic solvents just mentioned ethylene glycol possessed the strongest H-bond acidic character, followed by diethylene glycol, and finally 2-methoxyethanol. Hydrogen-bond basicity followed the same order. Our analysis further showed that the solubilizing-related properties of diethylene glycol were a long way from the properties of most of the common organic solvents, hence diethylene glycol represents a useful possible solvent with somewhat different solubilizing-related properties to the majority of common organic solvents used in commercial manufacturing processes.

In the present communication we extend our earlier considerations to include triethylene glycol, which is used as liquid desiccant for natural gas, and as a solvent for aromatic hydrocarbon and paraffinic hydrocarbons separations during petroleum refining, and as a solvent in textile dyeing. Infinite dilution activity coefficients ( $\gamma^\infty$ ) and gas-to-liquid partition coefficients were measured for 8 different liquid aliphatic and cyclic hydrocarbons (alkanes, cycloalkanes, alkynes), 9 different liquid aromatic compounds (benzene, alkylbenzenes, halobenzenes), 5 different liquid haloalkanes (dichloromethane, trichloromethane, 1-chlorobutane, 1,2-dichloropropane, isopropylbromide), acetone, tetrahydrofuran, 1,4-dioxane, butyl acetate, methanol, nitromethane and acetonitrile dissolved in triethylene glycol at 298.15 K using a headspace gas chromatographic method. Experimental molar solubilities were determined for anthracene, biphenyl, fluorene, 4-chlorobenzoic acid, 3,4-dichlorobenzoic acid, 4-methoxybenzoic acid, 3,4-dimethoxybenzoic acid, 2-methylbenzoic acid, 3-methylbenzoic acid, 2-methyl-3-nitrobenzoic acid, 2-chloro-5-

nitrobenzoic acid, 3-nitrobenzoic acid, 4-nitrobenzoic acid, 3,5-dinitrobenzoic acid, 3,5-dinitro-2-methylbenzoic acid, benzil, benzoin, 1,4-dibromobenzene, 1,4-dichloro-2-nitrobenzene, diphenyl sulfone, 9-fluorenone, 1-chloroanthraquinone, and xanthene dissolved in triethylene glycol at 298.15 K using a static equilibration-spectrophotometric method of analysis. Abraham model correlations for both water-to-triethylene glycol partition coefficients (as  $\log_{10} P$ ) and gas-to-triethylene glycol partition coefficients (as  $\log_{10} K$ ) were derived by combining our measured experimental data with published gas solubility and activity coefficient data for carbon dioxide [24], hydrogen sulfide [25], methane [26], ethane [26], propane [26], pentane [27], decane [28], dodecane [28], 2,2,4-trimethylpentane [29], cyclopentane [27], cyclohexane [29], cyclooctane [27], methylcyclohexane [29], ethylcyclohexane [29], 1-pentene [27], 1-hexene [27], 1-heptene [29], 1-octene [29], cis-2-hexene [28], 2,4,4-trimethyl-1-pentene [28], cyclohexene [29], 1-pentyne [27], 1-hexyne [27], propylbenzene [29], isopropylbenzene [29], 2-chloro-2-methylpropane [30], ethanol [27], 1-propanol [27], 2-propanol [27], and benzoic acid [31]. In total we have assembled experimental  $\log_{10} (C_{S,\text{organic}}/C_{S,\text{water}})$  and  $\log_{10} (C_{S,\text{organic}}/C_{S,\text{gas}})$  data for 82 different solutes to use in developing our Abraham model correlations.

## **Experimental Methodology**

### *Measurements of limiting activity coefficients of liquid organic solutes*

Triethylene glycol (Acros Organics, 99%), n-hexane (Sigma-Aldrich, 99%), n-heptane (Acros Organics, 99%), n-octane (Sigma-Aldrich, 99%), n-nonane (Acros Organics, 99%), n-undecane (Acros Organics, 99%), 1,7-octadiene (Acros Organics, 99%), 1-heptyne (Acros Organics, 99%), 1-octyne (Alfa Aesar, 98%), benzene (Komponent-Reaktiv, 99.8%), toluene (Sigma-Aldrich, 99.8%), ethylbenzene (Fluka, 99%), *o*-xylene (Sigma-Aldrich, 99%), *m*-xylene (Sigma-Aldrich, 99%), *p*-xylene (Sigma-Aldrich, 99%), fluorobenzene (Acros Organics, 99%),

chlorobenzene (Acros Organics, 99.6%), bromobenzene (Acros Organics, 99%), acetonitrile (J.T.Baker, 99.9%), butyl acetate (Ecos-1, 99.5%), dichloromethane (Kupavnareaktiv, 99.9%), trichloromethane (Component-Reactive, 99.85%), 1-chlorobutane (Acros Organics, 99.5%), 1,2-dichloropropane (Fluka, 98.5%), 2-bromopropane (Aldrich, 99%), tetrahydrofuran (Ecos-1, 99.5%), acetone (Ecos-1, 99.8%), methanol (Vekton, 99.5%), 1,4-dioxane (Komponent-Reaktiv, 99.5%), and nitromethane (Acros Organics, 99%) were purchased from commercial sources. They were used without further purification with the exceptions of tetrahydrofuran which was distilled over sodium. Purity of the substances was confirmed by their gas chromatograms showing no peaks with the area more than 0.5% of the main compound peak area and Karl Fisher titration (less than 100 ppm) proving the absence of significant amounts of water.

The measurements were conducted using gas chromatographic headspace analysis technique (Perkin Elmer Clarus 580 chromatograph with Turbomatrix HS-16 headspace autosampler). The samples of dilute solutions of the studied solutes in triethylene glycol as well as the pure solute samples were sealed in 22 ml vials, thoroughly shaken and thermostatted at 298.15 K. Samples of a small constant volume from the headspace of the vials were transferred by an autosampler into a gas chromatograph with HP-5 capillary column. The area of the chromatographic peak of a solute is proportional to its equilibrium vapor pressure  $p$  over a solution. In experiments with pure compounds, the peak area is proportional to the saturated vapor pressure of a pure solute  $p_{solute}^o$ . The activity coefficient at infinite dilution  $\gamma_\infty$  is given by  $\gamma_\infty = p / (p_{solute}^o \cdot x)$ , where  $x$  is the equilibrium molar fraction of a solute in the liquid phase. We correct the initial value of the molar fraction of a solute put into a vial by taking into account partial evaporation of a solute in order to obtain the value of  $x$  [14].

The working concentrations of solutes in triethylene glycol were 0.1–0.8 volume percents. For each solute, the results over 6 repetitions with different concentrations were averaged. No significant concentration dependence was observed, which proves that infinite dilution range is reached.

Logarithms of gas-to-liquid partition coefficients  $\log K$  are given by a formula  $\log_{10} K = \log_{10} \left( \frac{RT}{\gamma_{\infty} P_{solute}^{\circ} V_{solvent}} \right)$ , and the Gibbs free energy of solvation is calculated using a formula  $\Delta_{solv} G = RT \ln(\gamma_{\infty} P_{solute}^{\circ})$ . Standard states for  $K$  are unit concentration in mol dm<sup>-3</sup> in the gas phase and in solution, so that  $K$  has no units, while for  $\Delta_{solv} G$  we use a hypothetical ideal solution at unit mole fraction and a gas at 1 bar fugacity as the standard states. The values of  $P_{solute}^{\circ}$  at 298.15 K can be found in thermodynamic databases. The molar volume  $V_{solvent}$  of triethylene glycol is 133.4 ml·mol<sup>-1</sup>. Results are given in Table 1. Our values of limiting activity coefficients for several saturated and aromatic hydrocarbons are in good agreement with the results of Arancibia and Catoggio [29]. For other solutes, the values of  $\gamma_{\infty}$  in triethylene glycol at 298.15 K are reported for the first time.

Table 1. Limiting activity coefficients measured using gas chromatographic headspace analysis technique, gas-to-liquid partition coefficients, and the Gibbs free energies of solvation in triethylene glycol at  $T = 298.15$  K<sup>a</sup>

Solute	$\gamma_{\infty}$	$u(\gamma_{\infty})$	$\gamma_{\infty}$ (lit) [29]	$\text{Log}_{10} K$	$\Delta_{solv} G / (\text{kJ} \cdot \text{mol}^{-1})$
n-Hexane	61.0	2.0	67.0	1.180	6.2



n-Heptane	100	2.2	98.5	1.481	4.5
n-Octane	140	4.5	143	1.849	2.4
n-Nonane	218	4.7	208	2.157	0.6
n-Undecane	528	8.3		2.806	-3.1
1-Heptyne	11.1	0.2		2.378	-0.6
1-Octyne	15.6	0.2		2.817	-3.1
1,7-Octadiene	38.0	0.7		2.212	0.3
Benzene	3.45	0.20	3.80	2.629	-2.1
Toluene	5.50	0.26	6.01	2.950	-3.9
Ethylbenzene	8.84	0.30	9.31	3.215	-5.4
<i>o</i> -Xylene	8.02	0.19	8.68	3.419	-6.6
<i>m</i> -Xylene	9.23	0.22	9.89	3.260	-5.7
<i>p</i> -Xylene	9.23	0.25	9.85	3.232	-5.5
Fluorobenzene	2.85	0.09		2.801	-3.0
Chlorobenzene	3.10	0.11		3.573	-7.4
Bromobenzene	3.83	0.19		3.939	-9.5
Acetonitrile	1.12	0.02		3.146	-5.0
Butyl acetate	8.11	0.12		3.174	-5.2
Dichloromethane	0.92	0.04		2.542	-1.6
Chloroform	0.83	0.03		2.930	-3.8
n-Butyl chloride	8.40	0.07		2.215	0.3
1,2-Dichloropropane	2.82	0.09		2.967	-4.0
2-Bromopropane	5.98	0.06		2.032	1.4
Tetrahydrofuran	2.36	0.03		2.561	-1.7
Acetone	1.98	0.05		2.482	-1.2
Methanol	0.50	0.03		3.341	-6.1
1,4-Dioxane	1.69	0.05		3.335	-6.1
Nitromethane	1.07	0.04		3.561	-7.4

<sup>a</sup> Standard uncertainty for temperature  $u(T) = 0.2$  K.

*Measurements of solubilities of crystalline nonelectrolyte solutes*

Anthracene (Aldrich, 99+ %), benzil (Aldrich, 97 %), benzoin (Aldrich, 98 %), biphenyl (Aldrich, 99 %), 1-chloroanthraquinone (Aldrich, 98 %), 4-chlorobenzoic acid (Acros Organics, 99 %), 2-chloro-5-nitrobenzoic acid (Acros Organics, 99+ %), 1,4-dibromobenzene (Aldrich, 98 %), 1,4-dichloro-2-nitrobenzene (TCI America, 99+ %), 3,4-dichlorobenzoic acid (Aldrich, 99 %), 3,4-dimethoxybenzoic acid (Acros Organics, 99+ %), 3,5-dinitrobenzoic acid (Aldrich, 99+ %), 3,5-dinitro-2-methylbenzoic acid (Aldrich, 99+ %), diphenyl sulfone (Aldrich, 97 %), fluorene (Aldrich, 98 %), 9-fluorenone (Aldrich, 98 %), 4-methoxybenzoic acid (Aldrich, 99 %), 2-methylbenzoic acid (Aldrich, 99 %), 3-methylbenzoic acid (Aldrich, 99 %), 2-methyl-3-nitrobenzoic acid (Aldrich, 99 %), 3-nitrobenzoic acid (Aldrich, 99 %), 4-nitrobenzoic acid (Acros Organics, 99+ %), and xanthene (Aldrich, 98 %) were all purchased from commercial sources. Benzil, benzoin, xanthene, 1-chloroanthraquinone, 1,4-dibromobenzene, 1,4-dichloro-2-nitrobenzene, fluorene, and 9-fluorenone were recrystallized several times from anhydrous methanol prior to use. Anthracene was recrystallized several times from propanone. The recrystallized samples were dried for several days at 333 K prior to use. The remaining 14 solutes were used as received. Triethylene glycol (Sigma-Aldrich, 99 %) was stored for one week over activated molecular sieves and distilled shortly before use. Gas chromatographic analysis showed that the purity of triethylene glycol was 99.8 mass percent.

Solubilities were determined using a static equilibration method followed by a spectrophotometric determination of the concentration of dissolved solute in the saturated solutions based on the measured absorbance as described in our earlier publications [10, 32-53]. Our earlier papers describe the experimental methodology in great detail and to conserve journal

space the description will not be repeated here. Samples were allowed to equilibrate in a constant temperature bath at 298.15 K with periodic shaking for at least three days. Replicate measurements were performed two days after the original measurements to ensure that equilibrium had been reached. The concentration ranges and analysis wavelengths employed for each crystalline nonelectrolyte solute have also been reported in the afore-mentioned publications. To check for the possible formation of solid solvates we did remove and dry portions of the equilibrated solid phases after the solubility measurements were completed. Measured melting point temperatures of the recovered solid phase was within  $\pm 0.5$  K of the melting point temperature of the commercial sample or recrystallized solute prior to contact with triethylene glycol. Melting point studies indicated the absence of solid solvate formation.

Molar concentrations were converted into mole fraction solubilities using the mass of the sample aliquots taken for analysis, molar masses of triethylene glycol and the respective solutes, volume of the volumetric flasks, and any dilutions that were needed in order for the measured absorbances to fall on the Beer-Lambert law curve constructed from the absorbances of standard solutions.

Mole fraction solubilities of the 23 crystalline nonelectrolyte solutes dissolved in triethylene glycol that were measured as part of the present study are listed in Table 2. The numerical values represent the average of between four and eight independent experimental measurements. The reproducibility of the measured values was  $\pm 1.5$  % (relative error, smaller mole fraction solubilities) to  $\pm 2.5$  % (relative error, larger mole fraction solubilities). The slightly larger relative error for the solutes having the larger mole fraction solubilities results from the additional dilution needed to get the measured absorbances within the concentration range of the Beer-Lambert law curve. To our knowledge, this is the first time that the solubilities of these

solutes have been measured in triethylene glycol. The only solubility data that we found for solid solutes dissolved in triethylene glycol was the value for benzoic acid that was given in the Open Notebook Science Challenge [31].

Table 2. Experimental Mole Fraction Solubilities,  $X_{S,organic}^{exp}$ , of Crystalline Nonelectrolyte Solutes Dissolved in Triethylene Glycol at 298.15 K

Solute	$X_{S,organic}^{exp}$
Anthracene	0.00221
Benzil	0.0406
Benzoin	0.00894
Biphenyl	0.0588
1-Chloroanthraquinone	0.00389
4-Chlorobenzoic acid	0.0231
2-Chloro-5-nitrobenzoic acid	0.1463
1,4-Dibromobenzene	0.0256
3,4-Dichlorobenzoic acid	0.0215
1,4-Dichloro-2-nitrobenzene	0.1475
3,4-Dimethoxybenzoic acid	0.0337
3,5-Dinitrobenzoic acid	0.1266
3,5-Dinitro-2-methylbenzoic acid	0.1214
Diphenyl sulfone	0.0292
Fluorene	0.0238
9-Fluorenone	0.0768

4-Methoxybenzoic acid	0.0354
2-Methylbenzoic acid	0.1463
3-Methylbenzoic acid	0.1046
2-Methyl-3-nitrobenzoic acid	0.0765
3-Nitrobenzoic acid	0.1684
4-Nitrobenzoic acid	0.0388
Xanthene	0.0276

---

## Results and Discussion

The Abraham solvation parameter model, as noted above, can mathematically correlate solute transfer between two immiscible (or partly miscible) phases. Solute transfer properties can be described as water-to-organic solvent and gas-to-organic solvent partition coefficients, or as molar solubility ratios. Development of Abraham model correlations requires that one have a sufficient number of experimental partition coefficient values,  $\log_{10} P$  and  $\log_{10} K$  data, and molar solubility ratios,  $\log_{10} (C_{S,\text{organic}}/C_{S,\text{water}})$  and  $\log_{10} (C_{S,\text{organic}}/C_{S,\text{gas}})$  data, to perform meaningful regression analyses. The set(s) of partition coefficients and solubility ratios should include as diverse set of organic and inorganic solutes as possible so that the predictive area of chemical space defined by the range of solute descriptors is very large. This will increase the predictive applicability of the derived Abraham model correlations. For triethylene glycol we have performed headspace chromatographic measurements for the 29 different liquid organic solutes listed in Table 1. We have also measured the solubility of 23 different crystalline nonelectrolyte compounds dissolved in triethylene glycol. The list of crystalline compounds (see Table 2) includes several polycyclic aromatic hydrocarbons and carboxylic acids (hydrogen-bond donors

and hydrogen-bond acceptors), as well as several organic compounds that can act only as hydrogen-bond acceptors (e.g., benzil, 1-chloroanthraquinone, 9-fluorenone).

Our measured experimental values were augmented by experimental solubility data for several inorganic gases (carbon dioxide, hydrogen sulfide) and organic gases (methane, ethane, propane), and by experimental infinite dilution activity coefficient data for additional organic liquid solutes, that we found through our search of the published chemical and engineering data. The published Henry's law solubility data ( $K_{\text{Henry}}$ ) and published infinite dilution activity coefficient data ( $\gamma_{\infty}$ ) can be converted into  $\log_{10} P$  and  $\log_{10} K$  values through Eqns. 3 - 5 below:

$$\log_{10} K = \log_{10} \left( \frac{RT}{K_{\text{Henry}} V_{\text{solvent}}} \right) \quad (3)$$

$$\log_{10} K = \log_{10} \left( \frac{RT}{\gamma_{\infty} p_{\text{solute}}^{\circ} V_{\text{solvent}}} \right) \quad (4)$$

$$\text{Log}_{10} P = \log_{10} K - \log_{10} K_w \quad (5)$$

where  $R$  is the universal gas constant,  $T$  is the solution temperature (which for this communication is 298.15 K),  $p_{\text{solute}}^{\circ}$  is the vapor pressure of the solute at 298.15 K,  $V_{\text{solvent}}$  is the molar volume of triethylene glycol, and  $\log_{10} K_w$  is the logarithm of the solute's gas-to-water partition coefficient at 298.15 K. Tabulations of  $\log_{10} K_w$  are available in several of our earlier publications [54-57].

Partition coefficients and molar solubility ratios for solutes dissolved in a given solvent can be combined together into a single Abraham model correlation (see Eqns. 1 and 2). The experimental mole fraction solubility data tabulated in Table 2 are converted into molar solubilities by dividing  $X_{\text{S,organic}}^{\text{exp}}$  by the ideal molar volume of the saturated solution:

$$C_{\text{S,organic}}^{\text{exp}} \approx X_{\text{S,organic}}^{\text{exp}} / V_{\text{ideal soln}} \quad (6)$$

$$V_{\text{ideal soln}} = X_{\text{S,organic}}^{\text{exp}} V_{\text{Solute}} + (1 - X_{\text{S,organic}}^{\text{exp}}) V_{\text{Solvent}} \quad (7)$$

Numerical values of the molar volumes of the hypothetical subcooled liquid solutes were obtained by summing group values for the functional groups contained in the solute molecules. The molar solubility ratios of ( $C_{\text{S,organic}}/C_{\text{S,water}}$ ) and ( $C_{\text{S,organic}}/C_{\text{S,gas}}$ ) are obtained by dividing the solute's molar solubility in triethylene glycol by the solute's molar solubility in water,  $C_{\text{S,water}}$ , and by the solute's gas phase molar concentration,  $C_{\text{S,gas}}$ . Numerical values of  $C_{\text{S,water}}$  and  $C_{\text{S,gas}}$  are available in our earlier publications [10, 32-53] for all of the crystalline solutes considered in the current study. For most of the crystalline solutes the gas phase concentrations,  $C_{\text{S,gas}}$  were calculated at the time the solute descriptors were calculated. We have given in Table 3 the  $\log_{10}(P \text{ or } C_{\text{S,organic}}/C_{\text{S,water}})$  and  $\log_{10}(K \text{ or } C_{\text{S,organic}}/C_{\text{S,gas}})$  datasets that will be used to derive the Abraham model correlations for triethylene glycol. For the liquid and gaseous solutes the tabulated values correspond to partition coefficients for the respective solute dissolved in triethylene glycol. For the crystalline organic compounds the tabulated values represent the molar solubility ratios. Also included in the tabulation are the numerical values of the solute descriptors.

Table 3. Experimental  $\log_{10}(K \text{ or } C_{\text{S,organic}}/C_{\text{S,gas}})$  and  $\log_{10}(P \text{ or } C_{\text{S,organic}}/C_{\text{S,water}})$  Data for Solutes Dissolved in Triethylene Glycol at 298.15 K.

Solute	E	S	A	B	L	V	Log <sub>10</sub> K	Log <sub>10</sub> P	Ref
Carbon dioxide	0.000	0.280	0.050	0.100	0.058	0.2810	0.230	0.310	24
Hydrogen sulfide	0.350	0.310	0.100	0.070	0.723	0.2721	1.076	0.676	25
Methane	0.000	0.000	0.000	0.000	-0.323	0.2500	-0.987	0.473	26
Ethane	0.000	0.000	0.000	0.000	0.492	0.3900	-0.329	1.011	26
Propane	0.000	0.000	0.000	0.000	1.050	0.5313	0.031	1.471	26
Pentane	0.000	0.000	0.000	0.000	2.162	0.8130	0.796	2.496	27
Hexane	0.000	0.000	0.000	0.000	2.668	0.9540	1.180	3.000	This work
Heptane	0.000	0.000	0.000	0.000	3.173	1.0949	1.481	3.441	This work
Octane	0.000	0.000	0.000	0.000	3.677	1.2360	1.849	3.959	This work

Nonane	0.000	0.000	0.000	0.000	4.182	1.3767	2.157	4.307	This work
Decane	0.000	0.000	0.000	0.000	4.686	1.5180	2.422	4.742	28
Undecane	0.000	0.000	0.000	0.000	5.191	1.6590	2.806	5.186	This work
Dodecane	0.000	0.000	0.000	0.000	5.696	1.7990	3.125	5.655	28
2,2,4-Trimethylpentane	0.000	0.000	0.000	0.000	3.106	1.2360	1.383	3.503	29
Cyclopentane	0.263	0.100	0.000	0.000	2.477	0.7050	1.357	2.237	27
Cyclohexane	0.305	0.100	0.000	0.000	2.964	0.8454	1.669	2.569	29
Cyclooctane	0.413	0.100	0.000	0.000	4.329	1.1272	2.530	3.150	27
Methylcyclohexane	0.244	0.060	0.000	0.000	3.319	0.9863	1.811	3.061	29
Ethylcyclohexane	0.263	0.100	0.000	0.000	3.877	1.1272	2.210	3.790	29
1-Pentene	0.093	0.080	0.000	0.070	2.047	0.7700	0.990	2.220	27
1-Hexene	0.078	0.080	0.000	0.070	2.572	0.9110	1.391	2.551	27
1-Heptene	0.092	0.080	0.000	0.070	3.063	1.0520	1.676	2.906	29
1-Octene	0.094	0.080	0.000	0.070	3.568	1.1930	2.033	3.443	29
cis-2-Hexene	0.080	0.080	0.000	0.070	2.687	0.9110	1.474	2.634	28
2,4,4-Trimethyl-1-pentene	0.090	0.070	0.000	0.070	3.289	1.1928	1.717	3.187	28
1,7-Octadiene	0.191	0.200	0.000	0.100	3.415	1.1498	2.212	3.172	This work
Cyclohexene	0.395	0.200	0.000	0.070	3.021	0.8020	2.001	2.271	29
1-Pentyne	0.172	0.230	0.120	0.120	2.010	0.7271	1.638	1.648	27
1-Hexyne	0.166	0.220	0.100	0.120	2.510	0.8680	2.163	2.373	27
1-Heptyne	0.160	0.230	0.090	0.100	3.000	1.0089	2.378	2.818	This work
1-Octyne	0.155	0.220	0.090	0.100	3.521	1.1500	2.817	3.337	This work
Dichloromethane	0.390	0.570	0.100	0.050	2.019	0.4943	2.542	1.582	This work
Trichloromethane	0.425	0.490	0.150	0.020	2.480	0.6170	2.930	2.140	This work
1-Chlorobutane	0.210	0.400	0.000	0.100	2.722	0.7946	2.215	2.095	This work
2-Chloro-2-methylpropane	0.142	0.300	0.000	0.030	2.273	0.7946	1.824	2.624	30
1,2-Dichloropropane	0.370	0.630	0.000	0.170	2.836	0.7761	2.967	1.997	This work
Isopropylbromide	0.332	0.350	0.000	0.140	2.390	0.7063	2.032	1.682	This work
Benzene	0.610	0.520	0.000	0.140	2.786	0.7164	2.629	1.999	This work
Toluene	0.601	0.520	0.000	0.140	3.325	0.8573	2.950	2.300	This work
Ethylbenzene	0.613	0.510	0.000	0.150	3.778	0.9982	3.215	2.635	This work
Propylbenzene	0.604	0.500	0.000	0.150	4.230	1.1390	3.441	3.051	29
Isopropylbenzene	0.602	0.490	0.000	0.160	4.084	1.1390	3.348	2.908	29
<i>o</i> -Xylene	0.663	0.560	0.000	0.160	3.939	0.9982	3.419	2.759	This work
<i>m</i> -Xylene	0.623	0.520	0.000	0.160	3.839	0.9982	3.260	2.650	This work
<i>p</i> -Xylene	0.613	0.520	0.000	0.160	3.839	0.9982	3.232	2.642	This work
Tetrahydrofuran	0.289	0.520	0.000	0.480	2.636	0.6223	2.561	0.271	This work
1,4-Dioxane	0.329	0.750	0.000	0.640	2.892	0.6810	3.335	-0.375	This work
Acetone	0.179	0.700	0.040	0.490	1.696	0.5470	2.482	-0.348	This work
Butyl acetate	0.071	0.600	0.000	0.450	3.353	1.0284	3.174	1.234	This work
Acetonitrile	0.237	0.900	0.070	0.320	1.739	0.4042	3.146	0.296	This work



Methanol	0.278	0.440	0.430	0.470	0.970	0.3082	3.341	-0.399	This work
Ethanol	0.246	0.420	0.370	0.480	1.485	0.4491	3.262	-0.407	27
1-Propanol	0.236	0.420	0.370	0.480	2.031	0.5900	3.640	0.080	27
2-Propanol	0.212	0.360	0.330	0.560	1.764	0.5900	3.279	-0.201	27
Nitromethane	0.313	0.950	0.060	0.310	1.892	0.4237	3.561	0.611	This work
Anthracene	2.290	1.340	0.000	0.280	7.568	1.4544	7.674	4.643	This work
Fluorene	1.588	1.060	0.000	0.250	6.922	1.3565	6.696	4.246	This work
Biphenyl	1.360	0.990	0.000	0.260	6.014	1.3242	5.916	3.966	This work
Fluorobenzene	0.477	0.570	0.000	0.100	2.788	0.7341	2.801	2.211	This work
Chlorobenzene	0.718	0.650	0.000	0.070	3.657	0.8388	3.573	2.753	This work
Bromobenzene	0.882	0.730	0.000	0.090	4.041	0.8914	3.939	2.869	This work
1,4-Dibromobenzene	1.150	0.860	0.000	0.040	5.324	1.0660	4.789	3.349	This work
Xanthene	1.502	1.070	0.000	0.230	7.153	1.4152	7.020	4.520	This work
Benzoic acid	0.730	0.900	0.590	0.400	4.657	0.9317	7.088	1.948	31
3-Nitrobenzoic acid	0.990	1.180	0.730	0.520	5.601	1.1059	8.716	1.786	This work
4-Nitrobenzoic acid	0.990	1.520	0.680	0.400	5.770	1.1059	9.340	2.440	This work
3,5-Dinitrobenzoic acid	1.250	1.630	0.700	0.590	6.984	1.2801	10.691	2.391	This work
4-Methoxybenzoic acid	0.899	1.250	0.620	0.520	5.741	1.1313	8.920	2.220	This work
3,4-Dimethoxybenzoic acid	0.950	1.646	0.570	0.755	6.746	1.3309	10.339	1.892	This work
4-Chlorobenzoic acid	0.840	1.020	0.630	0.270	4.947	1.0541	7.595	2.795	This work
3,5-Dinitro-2-methylbenzoic acid	1.310	2.120	0.750	0.650	8.040	1.4210	12.505	2.548	This work
2-Methylbenzoic acid	0.730	0.840	0.420	0.440	4.677	1.0726	6.386	2.086	This work
3-Methylbenzoic acid	0.730	0.890	0.600	0.400	4.819	1.0726	7.014	2.034	This work
2-Chloro-5-nitrobenzoic acid	1.250	1.400	0.670	0.460	6.513	1.2283	9.575	2.625	This work
3,4-Dichlorobenzoic acid	0.950	0.920	0.670	0.260	5.623	1.1766	7.923	3.183	This work
2-Methyl-3-nitrobenzoic acid	1.040	1.396	0.541	0.532	6.332	1.2468	9.200	2.463	This work
Diphenyl sulfone	1.570	2.150	0.000	0.700	8.902	1.6051	10.363	2.973	This work
Benzoin	1.585	2.115	0.196	0.841	9.159	1.6804	11.221	2.490	This work
Benzil	1.445	1.590	0.000	0.620	7.611	1.6374	8.392	3.522	This work
1-Chloroanthraquinone	1.900	1.790	0.000	0.570	9.171	1.6512	10.034	4.000	This work
9-Fluorenone	1.600	1.490	0.000	0.350	7.474	1.3722	7.933	3.733	This work
1,4-Dichloro-2-nitrobenzene	1.120	1.289	0.000	0.199	5.783	1.1354	6.243	3.342	This work

There are more than enough experimental  $\log_{10}(P \text{ or } C_{S,\text{organic}}/C_{S,\text{water}})$  and  $\log_{10}(K \text{ or } C_{S,\text{organic}}/C_{S,\text{gas}})$  values for us to derive meaningful Abraham model correlations for solute transfer into triethylene glycol. Most of our published Abraham model correlations are based on between 35 to more than 100 experimental values. The solutes studied are chemically diverse and cover a wide range of polarity and hydrogen-bonding character as reflected in their solute descriptor

values. Regression analysis of the experimental values in Table 3 in accordance with Abraham model Eqns. 1 and 2 yielded the following two mathematical correlations:

$$\log_{10} (P \text{ or } C_{S,\text{organic}}/C_{S,\text{water}}) = -0.071(0.056) + 0.501(0.086) \mathbf{E} + 0.074(0.109) \mathbf{S} + 0.157(0.098) \mathbf{A} \\ - 3.957(0.167) \mathbf{B} + 3.106(0.060) \mathbf{V} \quad (8)$$

(with  $N = 82$ ,  $SD = 0.159$ ,  $R^2 = 0.985$ ,  $F = 1006$ )

$$\log_{10} (K \text{ or } C_{S,\text{organic}}/C_{S,\text{gas}}) = -0.469(0.032) + 0.235(0.069) \mathbf{E} + 2.079(0.083) \mathbf{S} + 3.824(0.073) \mathbf{A} \\ + 0.775(0.125) \mathbf{B} + 0.626(0.012) \mathbf{L} \quad (9)$$

(with  $N = 82$ ,  $SD = 0.119$ ,  $R^2 = 0.999$ ,  $F = 10347$ )

where the associated statistical information includes the number of experimental data used in deriving the correlation equation ( $N$ ), the standard deviation expressed in  $\log_{10}$  units ( $SD$ ), the squared correlation coefficient ( $R^2$ ), and the Fisher  $F$ -statistic ( $F$ ). The standard errors in the equation coefficients are given in parentheses immediately following the respective coefficient to which the standard error pertains. All regression analyses were performed using the IBM SPSS Statistical 22 commercial software.

Examination of the coefficients and their respective errors indicates the standard error for the  $s$ -coefficient in Eqn. 8 is larger than the coefficient itself. We did reanalyze the  $\log_{10} (P \text{ or } C_{S,\text{organic}}/C_{S,\text{water}})$  after eliminating the  $s_p \cdot \mathbf{S}$  term to see if a better correlation could be obtained.

Reanalysis of the experimental  $\log_{10} (P \text{ or } C_{S,\text{organic}}/C_{S,\text{water}})$  gave:

$$\log_{10} (P \text{ or } C_{S,\text{organic}}/C_{S,\text{water}}) = -0.072(0.056) + 0.549(0.048) \mathbf{E} + 0.170(0.096) \mathbf{A} \\ - 3.877(0.118) \mathbf{B} + 3.106(0.060) \mathbf{V} \quad (10)$$

(with  $N = 82$ ,  $SD = 0.160$ ,  $R^2 = 0.985$ ,  $F = 1267$ )

Very little loss in descriptive ability was observed by elimination of the  $s_p \cdot \mathbf{S}$  term. The standard deviations of Eqns. 8 and 10 were essentially identical,  $SD = 0.159 \log_{10}$  units versus  $SD = 0.160$

$\log_{10}$  units. The F-statistic did increase slightly from  $F = 1006$  to  $F = 1267$ , and the standard errors in the equation coefficients decreased slightly. From a predictive point-of-view both equations should provide comparable predictions of  $\log_{10} (P \text{ or } C_{S,\text{organic}}/C_{S,\text{water}})$  for additional solutes.

All three Abraham model correlations are statistically very good as evidenced by the relatively small standard deviations ( $SD = 0.159 \log_{10}$  units for Eqn. 8;  $SD = 0.119 \log_{10}$  units for Eqn. 9; and  $SD = 0.160 \log_{10}$  units for Eqn. 10) and near unity values for the squared correlation coefficients ( $R^2 = 0.985$ ;  $R^2 = 0.999$ ; and  $R^2 = 0.985$ ). Figure 1 compares the observed  $\log_{10} (K \text{ or } C_{S,\text{organic}}/C_{S,\text{gas}})$  values against the back-calculated values based on Eqn. 9. The experimental dataset covers an approximate range of  $13.5 \log_{10}$  units, from  $\log_{10} K = -0.987$  for methane to  $\log_{10} (C_{S,\text{organic}}/C_{S,\text{gas}}) = 12.505$  for 3,5-dinitro-2-methylbenzoic acid. A comparison of the back-calculated versus measured  $\log_{10} (P \text{ or } C_{S,\text{organic}}/C_{S,\text{water}})$  data is displayed in Figure 2 for Eqn. 10. The standard deviation for  $\log_{10} (P \text{ or } C_{S,\text{organic}}/C_{S,\text{water}})$  correlation are somewhat larger than that of the  $\log_{10} (K \text{ or } C_{S,\text{organic}}/C_{S,\text{gas}})$  correlations because the  $\log_{10} (P \text{ or } C_{S,\text{organic}}/C_{S,\text{water}})$  values contain the additional experimental uncertainty in the gas-to-water partition coefficients that were used in the  $\log_{10} (K \text{ or } C_{S,\text{organic}}/C_{S,\text{gas}})$  to  $\log_{10} (P \text{ or } C_{S,\text{organic}}/C_{S,\text{water}})$  conversions. Most of the data points in the datasets were based on experimental infinite dilution activity coefficients.

The predictive ability of Eqns. 8 - 10 were assessed by performing training set and test set analyses. The individual training and test sets were built by allowing the SPSS software to randomly select the experimental data points for one half of the compounds in the large datasets. The selected points were placed in the training sets and the remaining compounds were placed in the test sets. Analysis of the experimental  $\log_{10} (P \text{ or } C_{S,\text{organic}}/C_{S,\text{water}})$  and  $\log_{10} (K \text{ or } C_{S,\text{organic}}/C_{S,\text{gas}})$  data in the training sets yielded the following expressions:

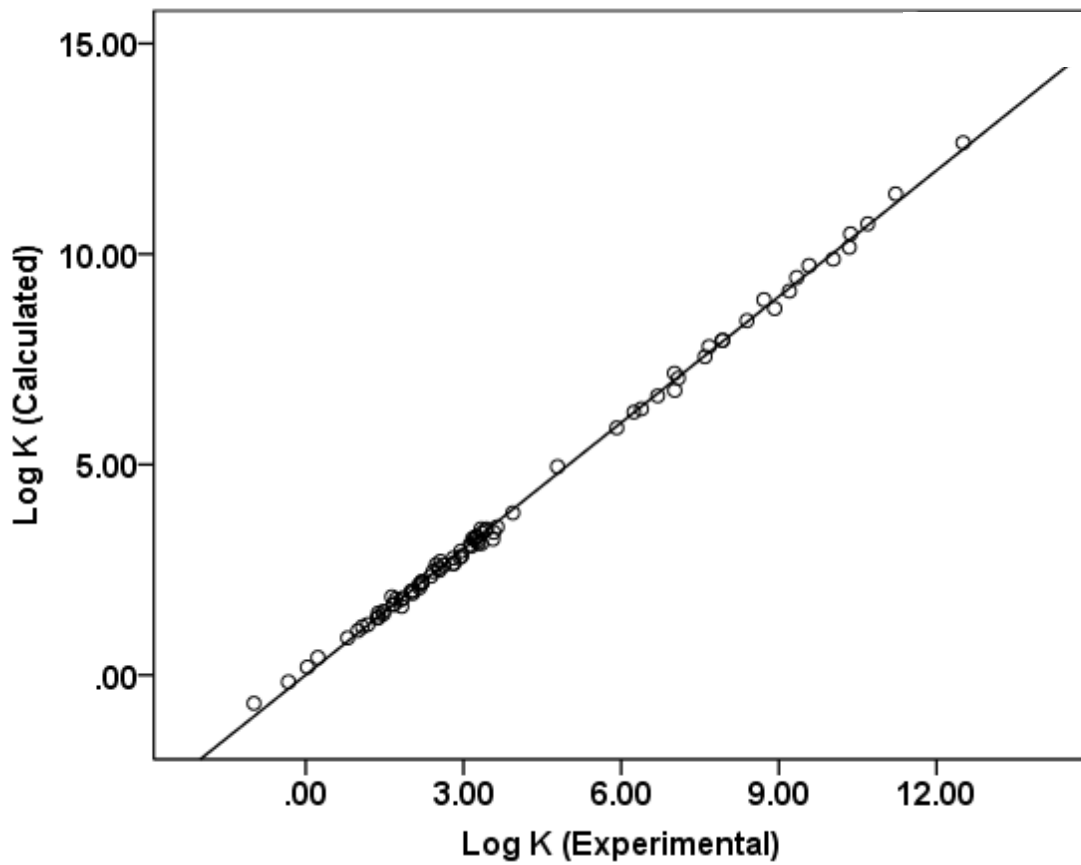


Figure 1. Comparison between experimental  $\log_{10}(K \text{ or } C_{S,\text{organic}}/C_{S,\text{gas}})$  values and calculated values based on Eqn. 9. In the case of the solid solutes the experimental and calculated values correspond to the logarithm of solubility ratios as denoted in Eqn. 9.

Figure 2

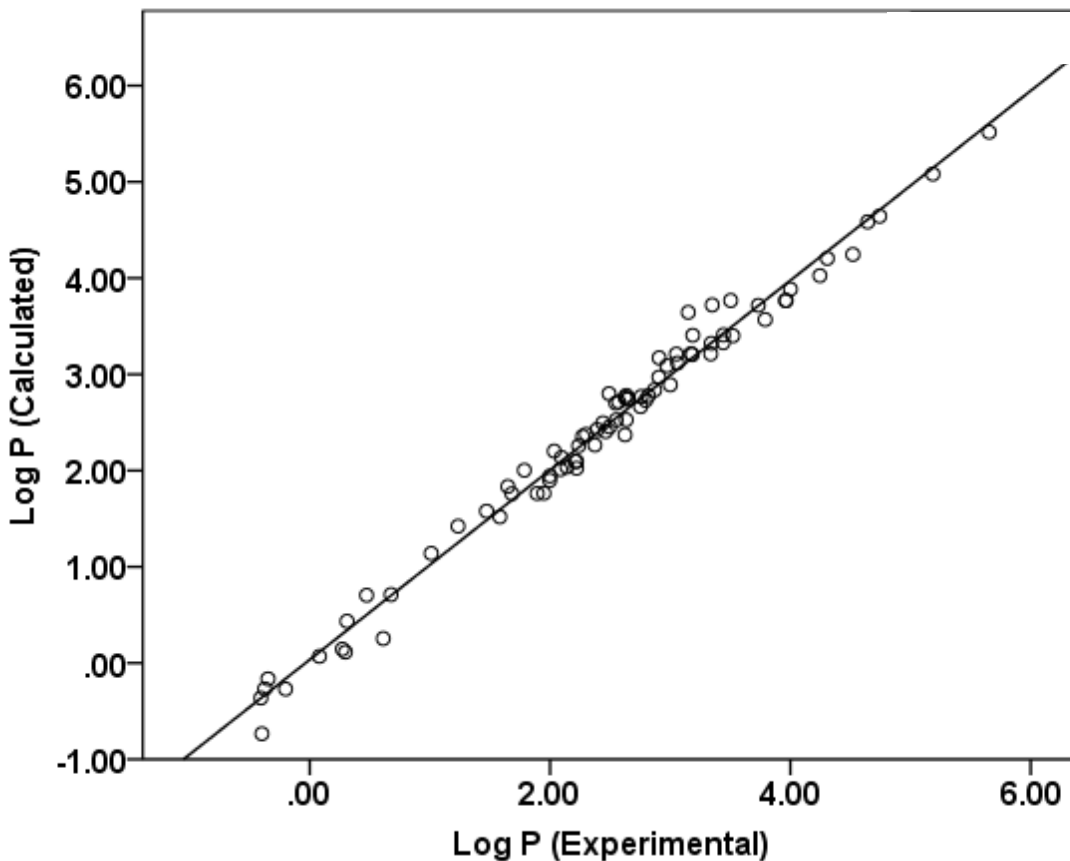


Figure 2. Comparison between experimental  $\log_{10} (P \text{ or } C_{S,\text{organic}}/C_{S,\text{water}})$  values and calculated values based on Eqn. 10. In the case of the solid solutes the experimental and calculated values correspond to the logarithm of solubility ratios as denoted in Eqn. 10.

$$\log_{10} (P \text{ or } C_{S,\text{organic}}/C_{S,\text{water}}) = -0.065(0.087) + 0.486(0.146) \mathbf{E} + 0.129(0.183) \mathbf{S} + 0.073(0.150) \mathbf{A} \\ - 4.044(0.288) \mathbf{B} + 3.111(0.092) \mathbf{V} \quad (11)$$

(with  $N = 41$ ,  $SD = 0.174$ ,  $R^2 = 0.983$ ,  $F = 412.3$ )

$$\log_{10} (P \text{ or } C_{S,\text{organic}}/C_{S,\text{water}}) = -0.070(0.086) + 0.572(0.081) \mathbf{E} + 0.085(0.147) \mathbf{A}$$

$$- 3.888(0.184) \mathbf{B} + 3.113(0.091) \mathbf{V} \quad (12)$$

(with  $N = 41$ ,  $SD = 0.174$ ,  $R^2 = 0.983$ ,  $F = 522.6$ )

$$\log_{10} (K \text{ or } C_{S,\text{organic}}/C_{S,\text{gas}}) = -0.445(0.051) + 0.271(0.119) \mathbf{E} + 2.091(0.140) \mathbf{S} + 3.772(0.113) \mathbf{A} \\ + 0.732(0.217) \mathbf{B} + 0.619(0.019) \mathbf{L} \quad (13)$$

(with  $N = 41$ ,  $SD = 0.131$ ,  $R^2 = 0.998$ ,  $F = 4245.6$ )

As before the  $\log_{10} (P \text{ or } C_{S,\text{organic}}/C_{S,\text{water}})$  correlations were determined with and without the  $s_p \cdot \mathbf{S}$  term. There is very little difference in the equation coefficients for the full dataset and the training dataset correlations, thus showing that both training sets of compounds are representative samples of the total  $\log_{10} (P \text{ or } C_{S,\text{organic}}/C_{S,\text{water}})$  and  $\log_{10} (K \text{ or } C_{S,\text{organic}}/C_{S,\text{gas}})$  data sets. The derived training set equations were then used to predict the respective partition coefficients for the compounds in the test sets. For the predicted versus experimental values, we found  $SD=0.160$  (Eqn. 11),  $SD = 0.159$  (Eqn. 12) and  $SD=0.119 \log_{10}$  units (Eqn. 13),  $AAE$  (average absolute error) =  $0.119$  (Eqn. 11),  $AAE = 0.118$  (Eqn. 12) and  $AAE=0.085 \log_{10}$  units (Eqn. 13), and  $AE$  (average error) =  $0.013$  (Eqn. 11),  $AE = 0.015$  (Eqn. 12) and  $AE=0.018 \log_{10}$  units (Eqn. 13). There is therefore very little bias in using Eqns. 11 - 13 with  $AE$  equal to  $0.013$ ,  $0.015$  and  $0.018 \log_{10}$  units. The training and test set analyses were conducted two more times with very similar results.

Previously [10] we have shown that the solvent properties of diethylene glycol were substantially different to those of most organic solvents, even those of alcohols, so that diethylene glycol represents a rather novel solvent. It is therefore of some interest to assess the solvent properties of triethylene glycol by comparison to diethylene glycol and general organic solvents. The easiest method is that of Principal Component Analysis, PCA. We list the five coefficients,  $e_k$ ,  $s_k$ ,  $a_k$ ,  $b_k$  and  $l_k$  in Eqn. 2, for a general selection of solvents in Table 4. Then application of PCA yields five PCs that are all orthogonal. The scores of the first two PCs contain most of the

information in the five equation coefficients, and a plot of PC2 against PC1 shows how near to each other are the PC points for the various solvents. Since the points are derived from the PC scores, which in turn are derived from equation coefficients, the distance between points then provides a visual assessment of how near the equations are in a chemical sense. The PC plot is depicted in Figure 3. It is immediately clear that triethylene glycol (No 1) and diethylene glycol (No 2) are very closely related and seem to form almost a separate solvent group as regards solubility related properties. This should not be unexpected as the Abraham model equation coefficients for triethylene glycol and diethylene glycol are very similar as evidenced by the first two lines of numerical entries in Table 4.

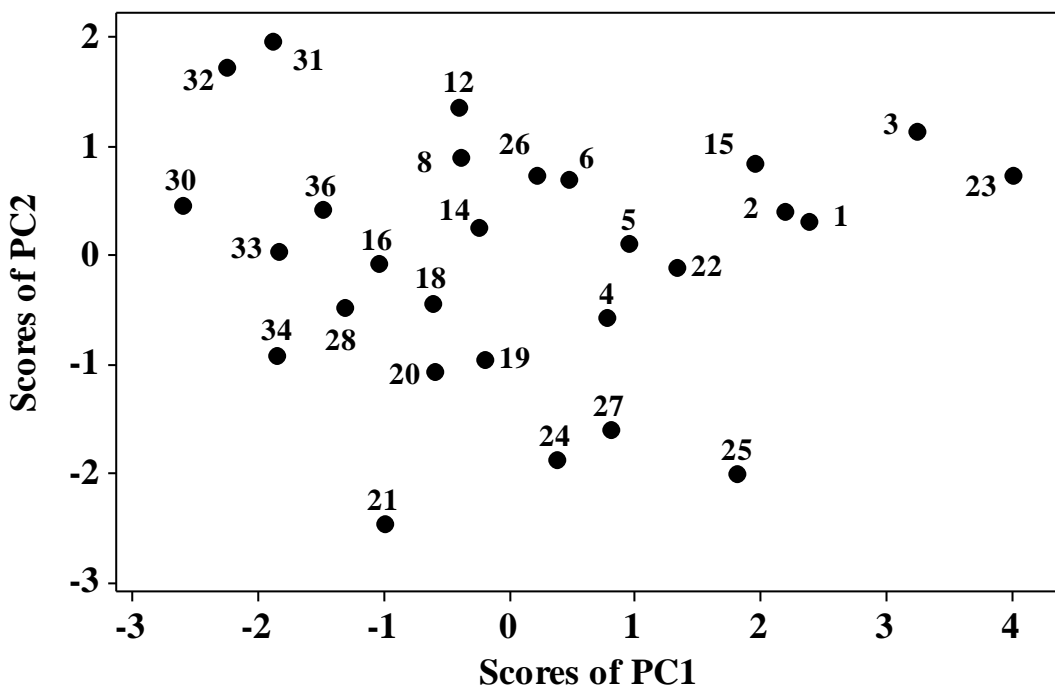


Figure 3. A plot of the scores of PC2 against the scores of PC1 for the equation coefficients given in Table 4. Points numbered as in Table 4. Some points have been left out to make the Figure clearer.

Table 4. Coefficients in Eqn. 2 for a selection of solvents.

Solvent	N	$c_k$	$e_k$	$s_k$	$a_k$	$b_k$	$l_k$
Triethylene glycol	1	-0.469	0.235	2.079	3.824	0.775	0.626
Diethylene glycol	2	-0.496	0.167	1.961	3.831	1.057	0.671
Ethylene glycol	3	-0.887	0.132	1.657	4.457	2.355	0.565
2-Methoxyethanol	4	-0.141	-0.265	1.810	3.641	0.590	0.790
Methanol	5	-0.039	-0.338	1.317	3.826	1.396	0.773
Ethanol	6	0.017	-0.232	0.867	3.894	1.192	0.846
Propan-1-ol	7	-0.042	-0.246	0.749	3.888	1.076	0.874
Octan-1-ol	8	-0.147	-0.214	0.561	3.507	0.749	0.943
Decan-1-ol	12	-0.139	-0.090	0.356	3.547	0.727	0.958
Propan-2-ol	13	-0.048	-0.324	0.713	4.036	1.055	0.884
t-Butanol	14	0.053	-0.443	0.699	4.026	0.882	0.907
Trifluoroethanol	15	-0.092	-0.547	1.339	2.213	3.807	0.645
Diethyl ether	16	0.288	-0.379	0.904	2.937	0.000	0.963
Dioxane	17	-0.034	-0.354	1.674	3.021	0.000	0.919
Ethyl acetate	18	0.182	-0.352	1.316	2.891	0.000	0.916
Propanone	19	0.127	-0.387	1.733	3.060	0.000	0.866
Butanone	20	0.112	-0.474	1.671	2.878	0.000	0.916
Dimethylformamide	21	-0.391	-0.869	2.107	3.774	0.000	1.011
N-Methylformamide	22	-0.249	-0.142	1.661	4.147	0.817	0.739
Formamide	23	-0.800	0.310	2.292	4.130	1.933	0.442
Acetonitrile	24	-0.007	-0.595	2.461	2.085	0.418	0.738
Dimethyl sulfoxide	25	-0.556	-0.223	2.903	5.037	0.000	0.719
Tributyl phosphate	26	0.097	-0.098	1.103	2.411	0.588	0.844
Propylene carbonate	27	-0.356	-0.413	2.587	2.207	0.455	0.719
Dichloromethane	28	0.192	-0.572	1.492	0.460	0.847	0.965
Trichloromethane	29	0.157	-0.560	1.259	0.374	1.333	0.976
Tetrachloromethane	30	0.217	-0.435	0.554	0.000	0.000	1.069
Octane	31	0.219	0.000	0.000	0.000	0.000	0.960
Cyclohexane	32	0.163	-0.110	0.000	0.000	0.000	1.013
Toluene	33	0.085	-0.400	1.063	0.501	0.154	1.011



Fluorobenzene	34	0.181	-0.621	1.432	0.647	0.000	0.986
Bromobenzene	35	-0.064	-0.326	1.261	0.323	0.292	1.002
Iodobenzene	36	-0.171	-0.192	1.197	0.245	0.245	1.002
Nitrobenzene	37	-0.296	0.092	1.707	1.147	0.443	0.912

## Conclusion

Expressions based on the Abraham solvation parameter model have been shown to give reasonably accurate mathematical descriptions of the solute transfer properties of a chemically diverse set of organic and inorganic solutes into triethylene glycol from both water and from the gas phase. The derived Abraham model correlations described the logarithms of the observed water-to-triethylene glycol partition coefficients, logarithms of the gas-to-triethylene glycol partition coefficients and logarithms of the molar solubility ratios to within 0.16  $\log_{10}$  units. Training and test set analyses indicated that the derived mathematical expressions should provide very good estimations of  $\log_{10} P$ ,  $\log_{10} K$ ,  $\log_{10} (C_{S,\text{organic}}/C_{S,\text{water}})$ , and  $\log_{10} (C_{S,\text{organic}}/C_{S,\text{gas}})$  for additional solutes dissolved in triethylene glycol, provided that the numerical values of the solute descriptors fall within the range of values used in determining the predictive expressions. Principal Component Analysis further showed that triethylene glycol (No 1) and diethylene glycol (No 2) are very closely related and seem to form almost a separate solvent group as regards their solubilization related properties. Despite very close solvation properties, in industrial applications such as natural gas desiccation and hydrocarbon separation, triethylene glycol and higher oligomers of ethylene glycol have an advantage over diethylene glycol due to their significantly lower volatility, leading to less vapor losses and easier regeneration.

## Acknowledgement

The work of Igor Sedov and Timur Magsumov was performed according to the Russian Government Program of Competitive Growth of Kazan Federal University. Maribel Barrera thanks the University of North Texas and the U.S. Department of Education for support provided under the Ronald E. McNair Postbaccalaureate Achievement Program.

## References

1. Byrne, F.P., Jin, S., Paggiola, G., Petchey, T.H.M., Clark, J.H., Farmer, T.J., Hunt, A.J., McElroy, C.R., Sherwood, J.: Tools and techniques for solvent selection: green solvent selection guide. *Sustainable Chem. Proc.* **4**, 7/1-7/24 (2016).
2. Dunn, P.J.: The importance of green chemistry in process research and development. *Chem. Soc. Reviews* **41**, 1452-1461 (2012).
3. Weis, D.C., Visco, D.P.: Computer-aided molecular design using the Signature molecular descriptor: Application to solvent selection. *Comp. Chem. Eng.* **34**, 1018-1029 (2010).
4. Henderson, R.K., Jimenez-Gonzalez, C., Constable, D.J C., Alston, S.R., Inglis, G.G.A., Fisher, G., Sherwood, J., Binks, S.P., Curzons, A.D.: Expanding GSK's solvent selection guide - embedding sustainability into solvent selection starting at medicinal chemistry. *Green Chem.* **13**, 854-862 (2011).
5. Lawrenson, S., North, M., Peigneguy, F., Routledge, A.: Greener solvents for solid-phase synthesis. *Green Chem.* **19**, 952-962 (2017).
6. Pacheco, A.A.C., Sherwood, J., Zhenova, A., McElroy, C.R., Hunt, A.J., Parker, H.L., Farmer, T.J., Constantinou, A., De Bruyn, M., Whitwood, A.C., Raverty, W., Clark, J.H.: Intelligent approach to solvent substitution: the identification of a new class of levoglucosenone derivatives. *ChemSusChem* **9**, 3503-3512 (2016).
7. Sathish, M., Silambarasan, S., Madhan, B., Raghava Rao, J.: Exploration of GSK'S solvent selection guide in leather industry: a CSIR-CLRI tool for sustainable leather manufacturing. *Green Chem.* **18**, 5806-5813 (2016).
8. Kralisch, D., Ott, D., Gericke, D.: Rules and benefits of Life Cycle Assessment in green chemical process and synthesis design: a tutorial review. *Green Chem.* **17**, 123-145 (2015).

9. Abraham, M.H., Smith, R.E., Luchtefeld, R., Boorem, A.J., Luo, R., Acree, W.E. Jr.: Prediction of solubility of drugs and other compounds in organic solvents. *J. Pharm. Sc.* **99**, 1500-1515 (2010).
10. Sedov, I.A., Magsumov, T.I., Hart, E., Higgins, E., Grover, D., Zettl, H., Zad, M., Acree, W.E. Jr., Abraham, M.H.: Abraham model expressions for describing water-to-diethylene glycol and gas-to-diethylene glycol solute transfer processes at 298.15 K. *J. Solution Chem.* **46**, 331-351 (2017).
11. Sedov, I.A., Salikov, T., Hart, E., Higgins, E., Acree, W.E. Jr., Abraham, M.H.: Abraham model linear free energy relationships for describing the partitioning and solubility behavior of nonelectrolyte organic solutes dissolved in pyridine at 298.15 K. *Fluid Phase Equilib.* **431**, 66-74 (2017).
12. Sedov, I.A., Khaibrakhmanova, D., Hart, E., Grover, D., Zettl, H., Koshevarova, V., Dai, C., Zhang, S., Schmidt, A., Acree, W.E. Jr., Abraham, M.H.: Development of Abraham model correlations for solute transfer into both 2-propoxyethanol and 2-isopropoxyethanol at 298.15 K. *J. Mol. Liq.* **212**, 833-840 (2015).
13. Hart, E., Grover, D., Zettl, H., Koshevarova, V., Zhang, S., Dai, C., Acree, W. E. Jr., Sedov, I.A., Stolov, M.A., Abraham, M.H.: Abraham model correlations for solute transfer into 2-methoxyethanol from water and from the gas phase. *J. Mol. Liq.* **209**, 738-744 (2015).
14. Sedov, I.A., Stolov, M.A., Hart, E., Grover, D., Zettl, H., Koshevarova, V., Dai, C., Zhang, S., Acree, W.E. Jr., Abraham, M.H.: Abraham model correlations for describing solute transfer into 2-butoxyethanol from both water and the gas phase at 298 K. *J. Mol. Liq.* **209**, 196-202 (2015).

15. Abraham, M.H., Acree, W.E. Jr.: Equations for the partition of neutral molecules, ions and ionic species from water to water-methanol mixtures. *J. Solution Chem.* **45**, 861-874 (2016).
16. Abraham, M.H., Acree, W.E. Jr.: Partition coefficients and solubilities of compounds in the water-ethanol solvent system. *J. Solution Chem.* **40**, 1279-1290 (2011).
17. Abraham, M.H., Acree, W.E. Jr.: Equations for the partition of neutral molecules, ions and ionic species from water to water-ethanol mixtures. *J. Solution Chem.* **41**, 730-740 (2012).
18. Jiang, B., Horton, M.Y., Acree, W.E. Jr., Abraham, M.H.: Ion-specific equation coefficient version of the Abraham model for ionic liquid solvents: determination of coefficients for tributylethylphosphonium, 1-butyl-1-methylmorpholinium, 1-allyl-3-methylimidazolium and octyltriethylammonium cations. *Phys. Chem. Liq.* **55**, 358-385 (2017).
19. Abraham, M.H.: Scales of solute hydrogen-bonding: their construction and application to physicochemical and biochemical processes. *Chem. Soc. Reviews* **22**, 73-83 (1993).
20. Abraham, M.H., Ibrahim, A., Zissimos, A.M.: Determination of sets of solute descriptors from chromatographic measurements. *J. Chromatog. A* **1037**, 29-47 (2004).
21. Clarke, E.D., Mallon, L.: The Determination of Abraham descriptors and their Application to Crop Protection Research. In: Jeschke, P., Kramer, W., Schirmer, U., Witschel M. (eds.) *Modern Methods in Crop Protection Research*, Wiley-VCH Verlag GmbH & Co. (2012).
22. Endo, S., Goss, K.-U.: Applications of polyparameter linear free energy relationships in environmental chemistry. *Environ. Sci. Technol.* **48**, 12477-12491 (2014).
23. Endo, S., Brown, T.N., Watanabe, N., Ulrich, N., Bronner, G., Abraham, M.H., Goss, K.-U.: UFZ-LSER database v 3.1 [Internet], Leipzig, Germany, Helmholtz Centre for

- Environmental Research-UFZ. 2015. Available from <http://www.ufz.de/lserd>. Accessed on March 17, 2017.
24. Fogg, P.G.T.: Carbon Dioxide in Non-aqueous Solvents at Pressures Less than 200 kPa, IUPAC Solubility Data Series, Vol. 50, Pergamon Press, Oxford, United Kingdom (1992).
  25. Fogg, P.G.T., Young, C.L.: Hydrogen Sulfide, Deuterium Sulfide and Hydrogen Selenide. IUPAC Solubility Data Series, Vol. 32, Pergamon Press, Oxford, United Kingdom (1988).
  26. Jou, F.Y., Deshmukh, R.D., Otto, F.D., Mather, A.E.: Vapor-liquid equilibria for acid gases and lower alkanes in triethylene glycol. *Fluid Phase Equilib.* **36**, 121-40 (1987).
  27. Williams-Wynn, M.D., Letcher, T.M., Naidoo, P., Ramjugernath, D.: Activity coefficients at infinite dilution of organic solutes in diethylene glycol and triethylene glycol from gas-liquid chromatography. *J. Chem. Thermodyn.* **65**, 120-130 (2013).
  28. Alessi, P.; Kikik, I., Tlustos G.: Activity coefficients of hydrocarbons in glycol. *Chim. Ind. Milan* **53**, 925-928 (1971).
  29. Arancibia, E.L., Catoggio, J.A.: Gas chromatographic study of solution and adsorption of hydrocarbons on glycols. I. Diethylene glycol and triethylene glycol. *J. Chromatog.* **197**, 135-145 (1980).
  30. Sedov I.A., Stolov M.A., Solomonov B.N.: Tert-butyl chloride as a probe of solvophobic effects. *Fluid Phase Equilib.* **382**, 164–168 (2014).
  31. Bradley, J.C.: Open notebook science challenge. [<http://onschallenge.wikispaces.com/>] Accessed on February 1, 2107.
  32. Acree, W.E. Jr., Abraham, M.H.: Solubility predictions for crystalline nonelectrolyte solutes dissolved in organic solvents based upon the Abraham general solvation model. *Can. J. Chem.* **79**, 1466-1476 (2001).

33. Roy, L.E., Hernandez, C.E., Acree, W.E. Jr.: Solubility of anthracene in organic nonelectrolyte solvents. Comparison of observed versus predicted values based upon mobile order theory (MOT). *Polycyclic Aromatic Compd.* **13**, 105-116 (1999).
34. Acree, W.E. Jr., Abraham, M.H.: Solubility predictions for crystalline polycyclic aromatic hydrocarbons (PAHs) dissolved in organic solvents based upon the Abraham general solvation model. *Fluid Phase Equilib.* **201**, 245-258 (2002).
35. Acree, W.E. Jr., Abraham, M.H.: Solubility of crystalline nonelectrolyte solutes in organic solvents: mathematical correlation of benzil solubilities with the Abraham general solvation model. *J. Solution Chem.* **31**, 293-303 (2002).
36. K. M. De Fina, K.M., Sharp, T.L., Acree, W.E. Jr.: Solubility of biphenyl in organic nonelectrolyte solvents. Comparison of observed versus predicted values based upon mobile order theory. *Can. J. Chem.* **77**, 1589-1593 (1999).
37. Stephens, T.W., Loera, M., Calderas, M., Diaz, R., Montney, N., Acree, W.E. Jr., Abraham, M.H.: Determination of Abraham model solute descriptors for benzoin based on measured solubility ratios. *Phys. Chem. Liq.* **50**, 254-265 (2012).
38. Flanagan, KB., Hoover, K.R., Garza, O., Hizon, A., Soto, T., Villegas, N., Acree, W.E. Jr.; Abraham, Michael H.: Mathematical correlation of 1-chloroanthraquinone solubilities in organic solvents with the Abraham solvation parameter model. *Phys. Chem. Liq.* **44**, 377-386 (2006).
39. Daniels, C.R., Charlton, A.K., Wold, R.M., Acree, W.E. Jr., Abraham, M.H.: Thermochemical behavior of dissolved carboxylic acid solutes: Solubilities of 3-methylbenzoic acid and 4-chlorobenzoic acid in organic solvents. *Can. J. Chem.* **81**, 1492-1501 (2003).

40. Stovall, D.M., Givens, C., Keown, S., Hoover, K.R., Barnes, R., Harris, C., Lozano, J., Nguyen, M., Rodriguez, E., Acree, W.E. Jr., Abraham, M.H.: Solubility of crystalline nonelectrolyte solutes in organic solvents: mathematical correlation of 4-chloro-3-nitrobenzoic acid and 2-chloro-5-nitrobenzoic acid solubilities with the Abraham solvation parameter model. *Phys. Chem. Liq.* **43**, 351-360 (2005).
41. Wilson, A., Tian, A., Chou, V., Quay, A.N., Acree, W.E. Jr., Abraham, M.H.: Experimental and predicted solubilities of 3,4-dichlorobenzoic acid in select organic solvents and in binary aqueous-ethanol mixtures. *Phys. Chem. Liq.* **50**, 324-335 (2012).
42. Brumfield, M., Wadawadigi, A., Kuprasertkul, N., Mehta, S., Stephens, T.W., Barrera, M., De La Rosa, J., Kennemer, K., Meza, J., Acree, W.E. Jr., Abraham, M.H.: Determination of Abraham model solute descriptors for three dichloronitrobenzenes from measured solubilities in organic solvents. *Phys. Chem. Liq.* **53**, 163-173 (2015).
43. Bowen, K.R., Stephens, T.W., Lu, H., Satish, K., Shan, D., Acree, W.E. Jr., Abraham, M.H.: Experimental and predicted solubilities of 3,4-dimethoxybenzoic acid in select organic solvents of varying polarity and hydrogen-bonding character. *Eur. Chem. Bull.* **2**, 577-583 (2013).
44. Hoover, K.R., Coaxum, R., Pustejovsky, E., Acree, W.E. Jr., Abraham, M.H.: Thermochemical behavior of dissolved carboxylic acid solutes: part 5-mathematical correlation of 3,5-dinitrobenzoic acid solubilities with the Abraham solvation parameter model. *Phys. Chem. Liq.* **42**, 457-466 (2004).
45. Ye, S., Saifullah, M., Grubbs, L.M., McMillan-Wiggins, M.C., Acosta, P., Mejorado, D., Flores, I., Acree, W.E. Jr., Abraham, M.H.: Determination of the Abraham model solute



- descriptors for 3,5-dinitro-2-methylbenzoic acid from measured solubility data in organic solvents, *Phys. Chem. Liq.* **49**, 821-829 (2011).
46. Fletcher, K.A., Hernandez, C.E., Roy, L.E., Coym, K.S., Acree, W.E. Jr.: Solubility of diphenyl sulfone in organic nonelectrolyte solvents. Comparison of observed versus predicted values based upon the general solvation model. *Can. J. Chem.* **77**, 1214-1217 (1999).
  47. Monarrez, C.I., Acree, W.E. Jr., Abraham, M.H.: Prediction and mathematical correlation of the solubility of fluorene in alcohol solvents based upon the Abraham general solvation model. *Phys. Chem. Liq.* **40**, 581-591 (2002).
  48. Stovall, D.M., Acree, W.E. Jr., Abraham, M.H.: Solubility of 9-fluorenone, thianthrene and xanthene in organic solvents, *Fluid Phase Equilibr.* **232**, 113-121 (2005).
  49. Hoover, K.R., Stovall, D.M., Pustejovsky, E., Coaxum, R., Pop, K., Acree, W.E. Jr., Abraham, M.H.: Solubility of crystalline nonelectrolyte solutes in organic solvents - mathematical correlation of 2-methoxybenzoic acid and 4-methoxybenzoic acid solubilities with the Abraham solvation parameter model. *Can. J. Chem.* **82**, 1353-1360 (2014).
  50. Coaxum, R., Hoover, K.R., Pustejovsky, E., Stovall, D.M., Acree, W.E. Jr., Abraham, M.H.: Thermochemical behavior of dissolved carboxylic acid solutes: Part 3 - Mathematical correlation of 2-methylbenzoic acid solubilities with the Abraham solvation parameter model. *Phys. Chem. Liq.* **42**, 313-322 (2004).
  51. Hart, E., Ramirez, A.M.; Cheeran, S., Barrera, M., Horton, M.Y.; Wadawadigi, A., Acree, W.E. Jr., Abraham, M.H.: Determination of Abraham model solute descriptors for 2-methyl-3-nitrobenzoic acid from measured solubility data in alcohol, alkyl ether, alkyl

- acetate and 2-alkoxyalcohol mono-solvents. *Phys. Chem. Liq.* (2017), Ahead of Print.  
DOI: 10.1080/00319104.2017.1283692
52. Charlton, A.K., Daniels, C.R., Wold, R., Pustejovsky, E., Acree, W.E. Jr., Abraham, M.H.: Solubility of crystalline nonelectrolyte solutes in organic solvents: mathematical correlation of 3-nitrobenzoic acid solubilities with the Abraham general solvation model. *J. Mol. Liq.* **116**, 19-28 (2004).
  53. Hoover, K.R., Coaxum, R., Pustejovsky, E., Stovall, D.M., Acree, W.E. Jr., Abraham, M.H.: Thermochemical behavior of dissolved carboxylic acid solutes: part 4 - mathematical correlation of 4-nitrobenzoic acid solubilities with the Abraham solvation parameter model. *Phys. Chem. Liq.* **42**, 339-347 (2004).
  54. Abraham, M.H., Acree, W.E. Jr., Cometto-Muniz, J.E.: Partition of compounds from water and from air into amides. *New J. Chem.* **33**, 2034-2043 (2009).
  55. Abraham, M.H., Acree, W.E. Jr., Leo, A.J., Hoekman, D.: Partition of compounds from water and from air into the wet and dry monohalobenzenes. *New J. Chem.* **33**, 1685-1692 (2009).
  56. Abraham, M.H., Acree, W.E., Leo, A.J., Hoekman, D.: The partition of compounds from water and from air into wet and dry ketones. *New J. Chem.* **33**, 568-573 (2009).
  57. Sprunger, L.M., Proctor, A., Acree, W.E. Jr., Abraham, M.H., Benjelloun-Dakhama, Nora.: Correlation and prediction of partition coefficient between the gas phase and water, and the solvents dry methyl acetate, dry and wet ethyl acetate, and dry and wet butyl acetate. *Fluid Phase Equilib.* **270**, 30-44 (2008).

## Glossary of Symbols and Definitions

### Lowercase alphabetical characters

$a_k$	solvent property in Eqn. 2 of the Abraham model reflecting the ability of the organic solvent to act as an H-bond acceptor
$a_p$	solvent property in Eqn. 1 of the Abraham model reflecting the ability of the organic solvent to act as an H-bond acceptor
$b_k$	solvent property in Eqn. 2 of the Abraham model reflecting the ability of the organic solvent to act as an H-bond donor
$b_p$	solvent property in Eqn. 2 of the Abraham model reflecting the ability of the organic solvent to act as an H-bond donor
$c_k$	constant in Eqn. 1 of the Abraham model
$c_p$	constant in Eqn. 1 of the Abraham model
$e_k$	solvent property in Eqn. 2 of the Abraham model reflecting the ability of the organic solvent to interact with dissolved solutes by electron lone pair interactions
$e_p$	solvent property in Eqn. 1 of the Abraham model reflecting the ability of the organic solvent to interact with dissolved solutes by electron lone pair interactions
$l_k$	solvent property in Eqn. 2 of the Abraham model describing the dispersion forces/cavity formation
$P_{solute}^o$	is the vapor pressure of the solute at 298.15 K
$s_k$	solvent property in Eqn. 2 of the Abraham model that reflects the dipolarity/polarizability of the organic solvent
$s_p$	solvent property in Eqn. 1 of the Abraham model that reflects the dipolarity/polarizability of the organic solvent
$v_p$	solvent property in Eqn. 1 of the Abraham model describing the dispersion forces/cavity formation

### Capitalized alphabetical characters

<b>A</b>	Abraham model solute descriptor corresponding to the overall or total hydrogen-bond acidity
<b>B</b>	Abraham model solute descriptor corresponding to the overall or total hydrogen-bond basicity

$C_{S,\text{gas}}$	molar gas phase concentration of the solute used in calculating the solubility ratio for Eqn. 2 of the Abraham model
$C_{S,\text{organic}}$	molar solubility of the solute in the organic solvent
$C_{S,\text{water}}$	molar solubility of the solute in water
<b>E</b>	solute descriptor corresponding to the solute excess molar refractivity in units of $(\text{cm}^3 \text{mol}^{-1})/10$ ,
$\Delta_{\text{solv}}G$	is the Gibbs energy of solvation of the solute
$K$	is the solute's gas-to-organic solvent partition coefficient
$K_w$	is the solute's gas-to-water partition coefficient at 298.15 K
<b>L</b>	is defined as the logarithm of the gas-to-hexadecane partition coefficient at 298 K.
$P$	is the solute's water-to-organic solvent partition coefficient
$R$	is the universal gas constant
<b>S</b>	Abraham model solute descriptor that quantifies the dipolarity/polarizability of the solute
$T$	is the system temperature in Kelvin
<b>V</b>	refers to the McGowan volume in units of $(\text{cm}^3 \text{mol}^{-1})/100$
$V_{\text{solute}}$	is the molar volume of the solute
$V_{\text{solvent}}$	is the molar volume of the solvent at 298.15 K
$X_{S,\text{organic}}^{\text{exp}}$	is the experimental mole fraction solubility of the solute in the organic solvent

#### Greek symbols

$\gamma_{\infty}$	is the infinite dilution activity coefficient of the solute
-------------------	---